Jurnal Geografi Gea

Journal homepage: https://ejournal.upi.edu/index.php/gea

# Comparative Analysis of DTM Extraction from Airborne LiDAR Point Cloud Data with Adaptive TIN Filter, Cloth Simulation Filter, and Progressive Morphological Filter Methods

*Panji Perkasa Sulung[1], Budhy Soeksmantono[2]*

*[1,2]Geodesy and Geomatics Study Program, Faculty of Earth Sciences and Technology, Institut Teknologi Bandung*
*Jln. Ganesha No. 10, Bandung 40132, Indonesia*

Correspondence e-mail: [1]25123017@mahasiswa.itb.ac.id, [2]soeksmantono@itb.ac.id

**ABSTRACT**

LiDAR, known for its high resolution and accuracy, is widely used in mapping applications. In addition, LiDAR can generate digital surface elevation data quickly and at a relatively affordable cost. However, raw LiDAR data cannot be directly processed into a Digital Terrain Model (DTM) because it still includes points from both ground and non-ground objects, making it necessary to separate the two through a filtering process to generate an accurate DTM. This study aims to compare the effectiveness of three filtering methods, namely Adaptive Triangulated Irregular Network (ATIN), Cloth Simulation Filter (CSF), and Progressive Morphological Filter (PMF) for extracting DTM from airborne LiDAR point cloud data. This research evaluates the performance of the three algorithms in handling various topographic conditions by reviewing relevant literature and conducting data processing. The study compares the filtered LiDAR point clouds and their resulting DTM representations. Results indicate that each filtering method has distinct strengths and limitations depending on the terrain and landscape characteristics. The findings provide insights into the selection of the most appropriate filtering algorithm for specific types of LiDAR point cloud data, thereby contributing to more accurate and efficient DTM generation in diverse geographical settings. These results offer practical implications for improving the precision of terrain mapping using LiDAR technology.

© 2025, FPIPS UPI. Open access article under the CC BY-SA license

**ARTICLE INFO**

***Article History:***
*Submitted/Received 27 June 2024*
*First Revised 12 July 2024*
*Accepted 25 April 2025*
*First Available online 30 April 2025*
*Publication Date 30 April 2025*

***Keyword:***
*LiDAR,*
*Point cloud,*
*Filtering,*
*DTM,*
*Representation,*
*Accuracy*

## 1. INTRODUCTION

Light Detection and Ranging (LiDAR) is an advanced remote sensing technology that measures the distance between an aerial vehicle and the Earth's surface (Kim et al., 2021). This measurement is done by emitting laser pulses and recording the time it takes each pulse to return after bouncing off the ground surface (Ramadhan et al., 2024; Hidayat dan Sudarsono, 2024). Typically, LiDAR systems are mounted on an Unmanned Aerial Vehicle (UAV), where they are integrated with the Global Positioning System (GPS) and an Inertial Measurement Unit (IMU) to precisely determine the coordinates of the vehicle's position during pulse emission (Lopac et al., 2022).

In recent years, LiDAR technology has become the preferred method for acquiring high-resolution elevation data of land surfaces (Samodra, 2022). This preference is driven by LiDAR's ability to generate high-quality digital surface elevation data rapidly and cost-effectively (Lin et al., 2021). The system records three-dimensional point cloud data, which can be utilized to create detailed Digital Elevation Model (DEM) essential for various surveying applications (Khan and Kumar, 2024). However, raw LiDAR data includes elevation points from various surface objects such as trees, buildings, and vehicles, making it unsuitable for direct conversion into DEM or Digital Terrain Model (DTM) without filtering (Oniga et al., 2023).

To generate accurate DEM/DTM data, it is necessary to filter the raw LiDAR data to remove points reflected from non-ground objects (Anand et al., 2021). This process involves interpolating the remaining ground points to produce a clearer representation of the terrain surface (Asy'ari et al., 2022). One of the primary challenges in LiDAR mapping is selecting the appropriate algorithm to separate ground points from non-ground points in the point cloud data. Numerous filtering algorithms exist, each with varying effectiveness depending on the specific conditions of the surveyed area (Fareed et al., 2023). Consequently, extensive experimentation is required to identify the optimal algorithm for particular scenarios (Chen et al., 2021).

The first notable filtering method is Adaptive Triangulated Irregular Network (ATIN), which uses iterative triangle subdivisions to smooth the terrain surface (Wang et al., 2021). This division is adaptive based on surface curvature, ensuring that areas with high curvature, such as mountains and valleys, are more finely divided compared to flatter areas (Zheng et al., 2024). The second method is Cloth Simulation Filter (CSF), which simulates a cloth draping over the landscape to identify ground points (Kuçak and Büyüksalih, 2023). By analyzing the interaction between the simulated cloth and the LiDAR points, the CSF can classify points based on their position relative to the final shape of the cloth (Bailey et al., 2022; Kim et al., 2021). The third method Progressive Morphological Filter (PMF), which progressively removes non-ground points using morphological operations. Using dilation and erosion operations, PMF iteratively removes non-ground objects from the LiDAR data by adjusting the filter window size until all non-ground objects are eliminated (Štroner et al., 2021). While these methods have been tested in different contexts, there is still a need for a comprehensive comparison of their performance across varying topographic conditions.

Previous studies have highlighted the strengths of these algorithms individually, but no consensus exists on their comparative effectiveness in diverse terrains. For example, ATIN excels in high-density point data but may struggle in flatter areas, while CSF and PMF offer flexible solutions but are sensitive to terrain complexity (Raj et al., 2024; Cai et al., 2023; Chen et al., 2021). This study fills the gap by directly comparing the three filtering methods namely ATIN, CSF, and PMF across different landscapes to determine their suitability for DTM extraction.

The aim of this study is to filter airborne LiDAR point cloud data using these three methods, generate DTMs, and evaluate the optimal conditions for each algorithm. The scope includes a detailed analysis of filtering performance in relation to terrain types, point cloud density, and the effectiveness of each method in producing accurate DTMs. The results will provide LiDAR data analysts with insights into selecting the most appropriate filtering method for specific use cases,

DOI: https://doi.org/10.17509/gea.v25i1.71587
p-ISSN 1412-0313 e- ISSN 2549-7529

ultimately enhancing LiDAR data processing for environmental monitoring, urban planning, and other applications requiring precise topographic data.

## 2. METHODS

This research utilizes LiDAR point cloud data acquired in May 2016 over the East Java area using a Leica ALS80 LiDAR sensor. The integration of the LiDAR sensor with the Differential GPS (DGPS) system on the aerial vehicle ensures that the acquired LiDAR point cloud data is referenced to the Zone 49S UTM coordinate system with the SRGI2013 datum, precisely aligned with the study area. Five distinct LiDAR point cloud datasets were employed, encompassing two separate study areas. The study areas are illustrated in Figure 1. The study areas feature diverse landscapes, including oil refinery zones, residential areas, rice fields, and densely vegetated hills, presenting challenges for ground filtering.

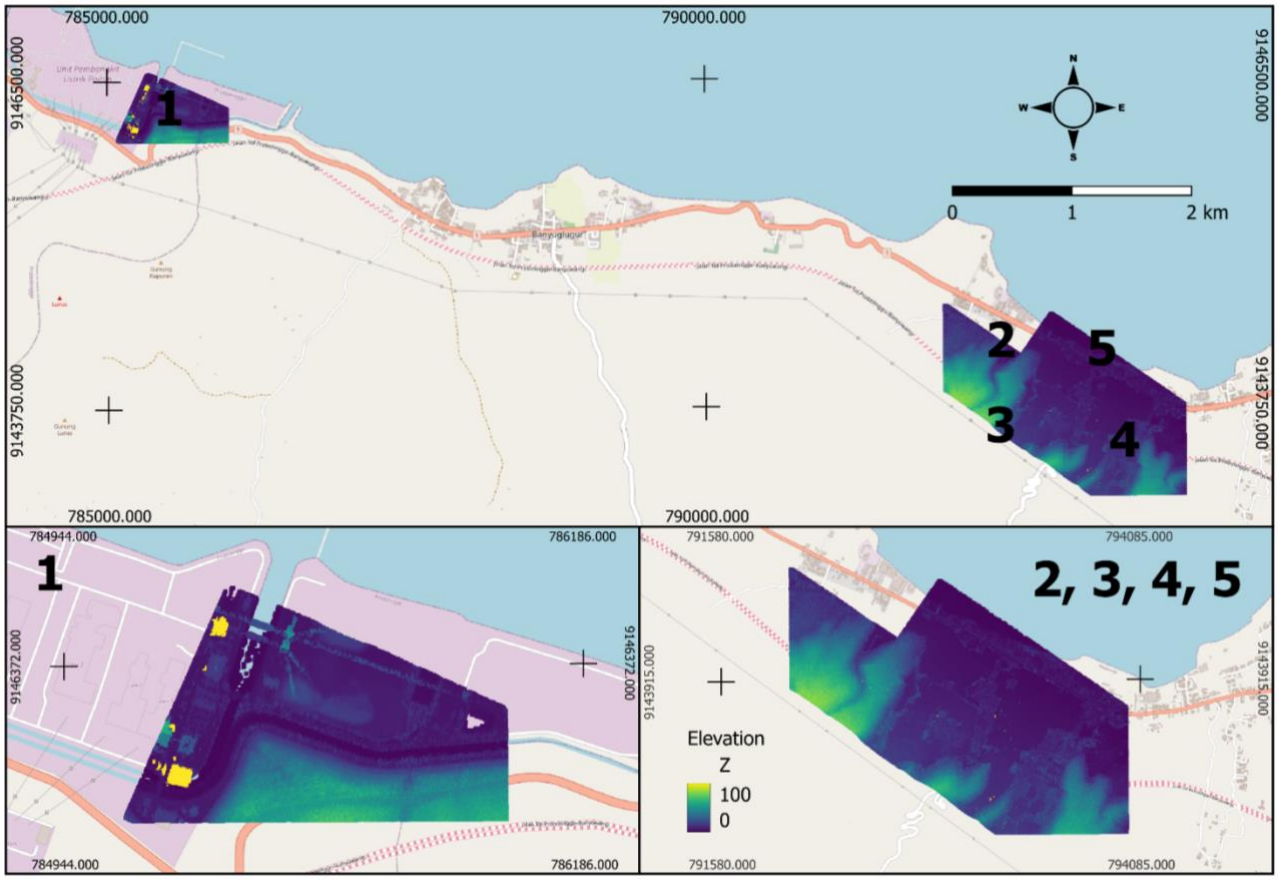


**Figure 1.** The Study Area

In addition to the LiDAR sensors, the DGPS and IMU systems were used to pinpoint the aerial vehicle's position during data acquisition. Metric cameras, specifically the Leica RCD30, were also employed to capture aerial photographs. These photographs are crucial in the data processing stage, serving as validators for the LiDAR point cloud data filtering results. The Leica RCD30's metric camera system was chosen for its ability to produce precise and accurate aerial photos, making it ideal for mapping purposes.

The data processing stage is broadly divided into four main processes: the Airborne LiDAR point cloud data filtering process, the checkpoint stereoplotting process, the DTM creation process, and the accuracy test process. The data processing workflow is outlined in Figure 2.

DOI: https://doi.org/10.17509/gea.v25i1.71587
p-ISSN 1412-0313 e- ISSN 2549-7529

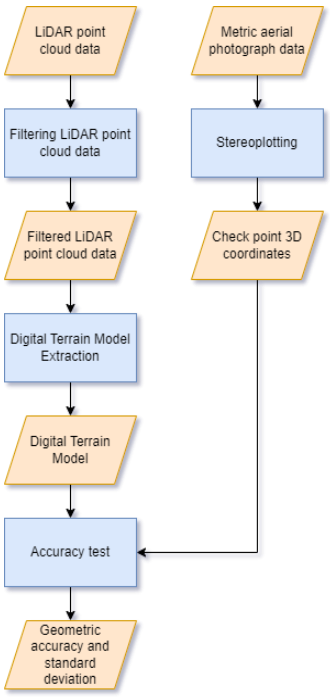


**Figure 2.** Data Processing Workflow

## 2.1 Filtering Process

The first stage involves filtering the LiDAR point cloud data using three different, widely-recognized methods, each with specific parameters to optimize their respective algorithms.

### *2.1.1 Adaptive Triangulated Irregular Network (ATIN) Method*

- The ATIN method is a filtering method that creates a TIN surface by connecting points and utilizing the distance between points on the TIN surface to select points on the ground. This algorithm is performed iteratively where the TIN surface is gradually compacted at each iteration (Li et al., 2021).
- Parameters:
  - Maximum Building Size: Determines the reference point for the largest object in the dataset.
  - Terrain Angle: Sets the slope alignment for the TIN triangles with the dataset surface.
  - Iteration Angle: Defines the maximum angle between a point and its projection on the TIN surface.
  - Iteration Distance: Specifies the maximum distance from a point to the TIN surface.

### *2.1.2 Cloth Simulation Filter (CSF) Method*

- The CSF method is a filtering method based on the cloth simulation technique, where a ground surface is turned over and then a piece of cloth is dropped in the hope that the cloth can produce a final shape that resembles the DTM surface (Yu et al., 2022).
- Parameters:
  - Data Characteristics: Determines the nature of the terrain (steep slope, relief, flat).
  - Cloth Resolution: Grid size of the cloth covering the data surface.
  - Maximum Iterations: Maximum number of simulation iterations.
  - Classification Threshold: Threshold for classifying ground and non-ground points based on distance from the cloth surface.

DOI: https://doi.org/10.17509/gea.v25i1.71587
p-ISSN 1412-0313 e- ISSN 2549-7529

*2.1.3 Progressive Morphological Filter (PMF) Method*

- The PMF method is a morphology-based LiDAR point cloud data filtering method that calculates the elevation difference between cells in a filter window that increases gradually in size in each iteration (Štroner et al., 2021).
- Parameters:
  - Cell Size: Size of cells for erosion and dilation operations.
  - Slope: Determines the threshold for elevation differences.
  - Initial and Maximum Thresholds: Defines the initial and maximum values for the elevation difference threshold.

**2.2 DTM Creation Process**

Post-filtering, the filtered points are used to create the DTM. The DTM extraction is carried out using the Binning method, which involves dividing the LiDAR point cloud data into fixed-size cells and using the points in each cell to generate a grid surface representing the ground.

**2.3 Checkpoint Stereo Plotting Process**

The stereoplotting process involves observing pairs of overlapping aerial photographs (stereo observation) using special glasses and monitors capable of displaying 3D images. This technique enables the extraction of three-dimensional position information of points on the Earth's surface, referred to as checkpoints, which are essential for the subsequent accuracy test stage. Coordinates of all checkpoints are saved after the stereoplotting process.

**2.4 Accuracy Test Process**

The accuracy test aims to evaluate two key metrics: geometric accuracy and standard deviation. Geometric accuracy measures the conformity between the vertical position (height) of points in the LiDAR dataset and their corresponding checkpoints from stereo observation. Higher geometric accuracy indicates minimal height differences, reflecting the effectiveness of the filtering method. Standard deviation quantifies the distribution of geometric accuracy values within the dataset. A smaller standard deviation indicates uniform accuracy, while a larger value suggests greater variation. Calculating the standard deviation of geometric accuracy values helps assess the consistency of the filtering method.

This research's comprehensive approach ensures a thorough evaluation of filtering methods, providing valuable insights and recommendations for optimizing LiDAR data processing in diverse and challenging terrains.

**3. RESULTS AND DISCUSSION**

The results of the LiDAR point cloud data filtering processing are point cloud data that has been classified as a land object and a non-land object, where points classified as non-land objects are removed in this filtering process. Based on the experiments that have been carried out, it is known that the parameters contained in each algorithm have an optimal range of values for each dataset. The value of each parameter used to perform the filtering process on each dataset can be seen in Table 1. The filtering process is then run with the optimal parameter combination for each dataset.

**Table 1.** Parameter Values for Each Algorithm

| Dataset | Algorithm | Parameters |
|---|---|---|
| 1 | ATIN | Max Building Size: 60 m; Terrain Angle: 88°; Iteration Angle: 10°; Iteration Distance: 0.5 m |
| | CSF | Scene: Relief; Cloth Resolution: 0.7; Max Iteration: 500; Classification Threshold: 0.5 |

DOI: https://doi.org/10.17509/gea.v25i1.71587
p-ISSN 1412-0313 e- ISSN 2549-7529

| | | |
|---|---|---|
| | PMF | Cell Size: 1 m; Slope: 0.5°; Initial Threshold: 0.05 m; Maximum Threshold: 100 m |
| 2 | ATIN | Max Building Size: 50 m; Terrain Angle: 88°; Iteration Angle: 10°; Iteration Distance: 0.5 m |
| | CSF | Scene: Relief; Cloth Resolution: 0.5; Max Iteration: 500; Classification Threshold: 0.5 |
| | PMF | Cell Size: 1 m; Slope: 0.5°; Initial Threshold: 0.05 m; Maximum Threshold: 100 m |
| 3 | ATIN | Max Building Size: 50 m; Terrain Angle: 88°; Iteration Angle: 10°; Iteration Distance: 0.5 m |
| | CSF | Scene: Relief; Cloth Resolution: 0.5; Max Iteration: 500; Classification Threshold: 0.5 |
| | PMF | Cell Size: 1 m; Slope: 0.6°; Initial Threshold: 0.1 m; Maximum Threshold: 100 m |
| 4 | ATIN | Max Building Size: 50 m; Terrain Angle: 88°; Iteration Angle: 9°; Iteration Distance: 0.5 m |
| | CSF | Scene: Relief; Cloth Resolution: 0.9; Max Iteration: 500; Classification Threshold: 0.5 |
| | PMF | Cell Size: 1 m; Slope: 0.6°; Initial Threshold: 0.1 m; Maximum Threshold: 100 m |
| 5 | ATIN | Max Building Size: 60 m; Terrain Angle: 88°; Iteration Angle: 4°; Iteration Distance: 0.5 m |
| | CSF | Scene: Flat; Cloth Resolution: 0.7; Max Iteration: 500; Classification Threshold: 0.5 |
| | PMF | Cell Size: 1 m; Slope: 0.1°; Initial Threshold: 0.1 m; Maximum Threshold: 100 m |

The results of the filtering process can be seen in Table 2, where the results are visualized in the top view. In the visualization of the filtering results, it can also be seen that each result has a different color gradation. The color gradation is based on the height difference between points, where the point with the lowest height is visualized in blue, while the point with the highest height is visualized in red.

**Table 2.** Point Cloud Filtering Results

| Dataset | Filtering Results | | |
|---|---|---|---|
| | ATIN | CSF | PMF |
| 1 | 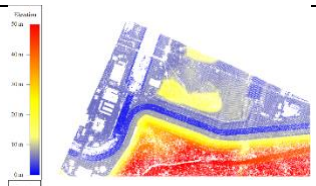 |  | 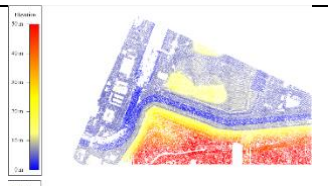 |
| 2 |  |  | 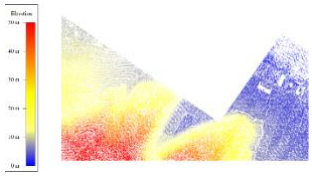 |

DOI: https://doi.org/10.17509/gea.v25i1.71587
p-ISSN 1412-0313 e- ISSN 2549-7529

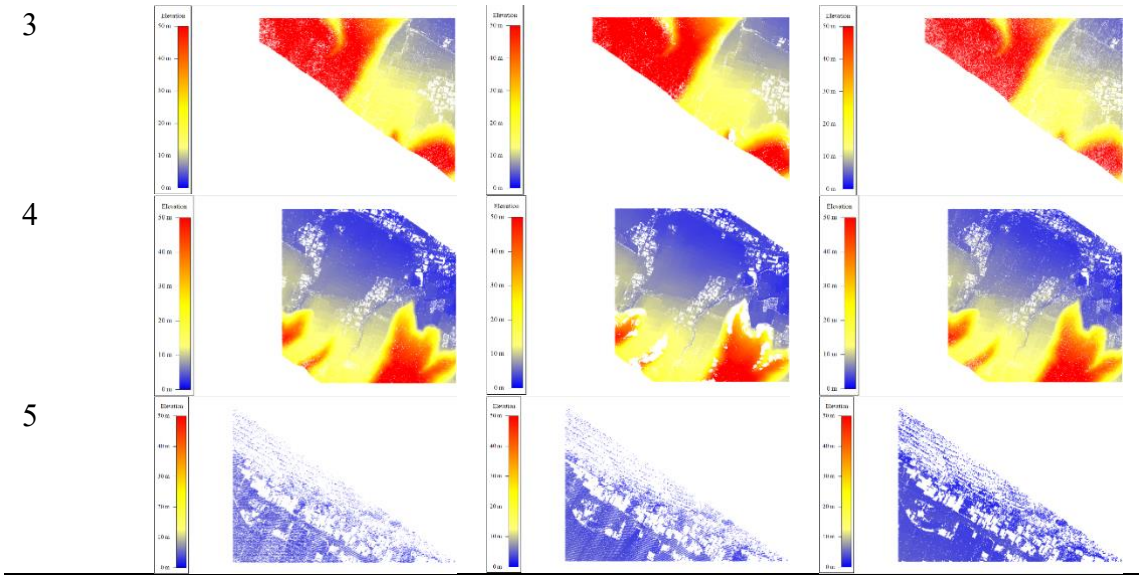


After obtaining the visualization results of the LiDAR point cloud data filtering process, the next step is to calculate the percentage of filtered points or points that are included in non-soil objects so that they are deleted during the filtering process. The percentage can be seen in Table 3.

**Table 3.** Percentage of Filtered Point Clouds

| Dataset | Percentage of Filtered Points (%) | | |
|---|---|---|---|
| | ATIN | CSF | PMF |
| 1 | 69.992 | 66 | 94.116 |
| 2 | 82.283 | 53 | 95.113 |
| 3 | 81.727 | 44 | 94.627 |
| 4 | 81.701 | 46 | 94.476 |
| 5 | 84.498 | 55 | 94.201 |

In addition to calculating the percentage of filtered points, the processing time of each algorithm was also calculated. Processing time is one of the important parameters to consider in LiDAR data processing. Table 4 shows the details of the time required for each method in performing the filtering process.

**Table 4.** Processing Time of LiDAR Data Filtering

| Dataset | Time Required (s) | | | Processed Points |
|---|---|---|---|---|
| | ATIN | CSF | PMF | |
| 1 | 6 | 23 | 19 | 3,469,177 |
| 2 | 4 | 19 | 47 | 4,408,593 |
| 3 | 12 | 83 | 34 | 6,254,334 |
| 4 | 24 | 13 | 68 | 12,326,774 |
| 5 | 1 | 3 | 5 | 998,564 |

It can be seen that the time taken to perform the filtering process in each method varies and does not always depend on the number of points processed alone. There are other factors that can affect the filtering processing time of LiDAR data such as file size to the selection of parameters used.

DOI: https://doi.org/10.17509/gea.v25i1.71587
p-ISSN 1412-0313 e- ISSN 2549-7529

Furthermore, each LiDAR data resulting from the filtering process in each method will be processed and extracted into a DTM, resulting in a total of 15 different DTMs whose visualizations can be seen in Table 5. The color gradation in the DTM extraction results is based on the height difference between points, where points with low altitude such as rice fields are visualized in blue, while points with high altitude such as hills are visualized in orange to red.

**Table 5.** DTM Extraction Results

| Dataset | DTM Representation | | |
|---|---|---|---|
| | ATIN | CSF | PMF |
| 1 | 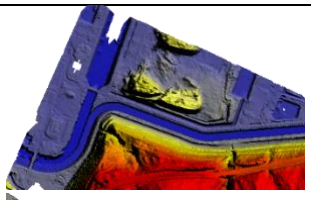 | 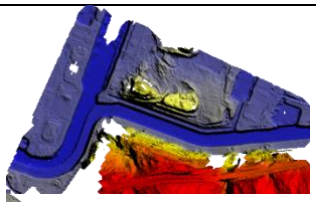 | 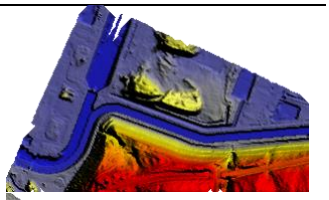 |
| 2 | 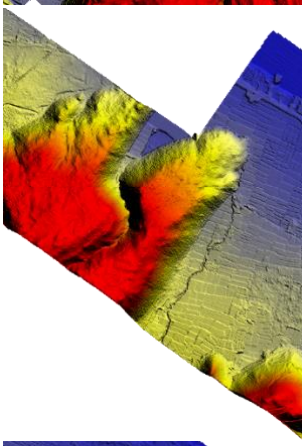 | 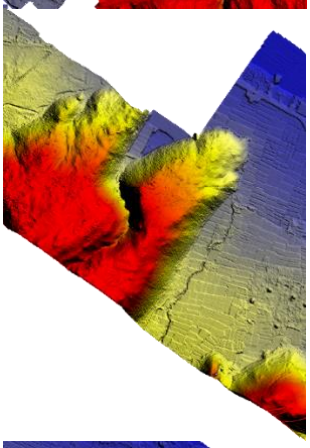 | 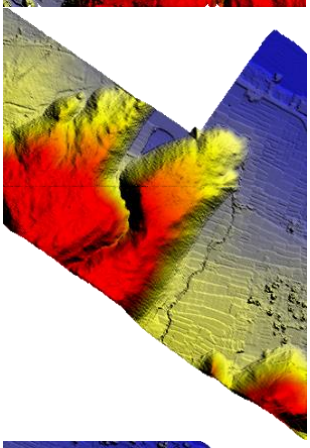 |
| 3 | | | |
| 4 | 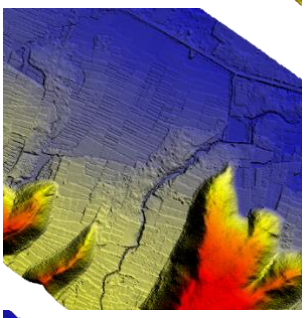 | 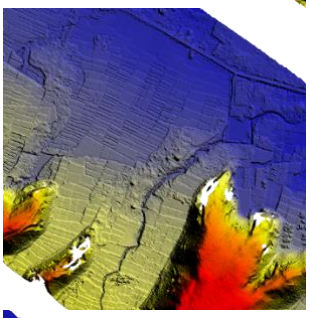 | 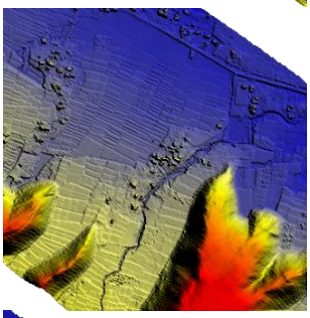 |
| 5 | 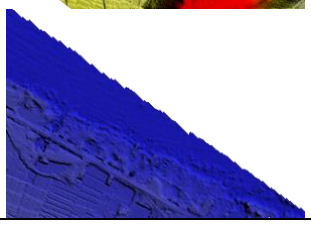 | 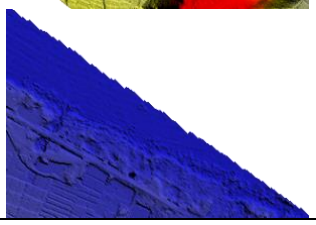 | 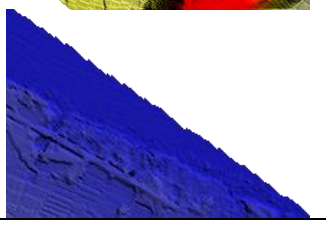 |

The three LiDAR datasets that have gone through the filtering process using the three methods can produce DTM surfaces with a fairly high resolution of 2 meters. This shows that LiDAR point cloud data can produce DTM surfaces with high resolution.

An accuracy test was then conducted to obtain the geometric accuracy and standard deviation in the LiDAR dataset, referring to the check point coordinates obtained through the stereoplotting process of the metric aerial photography data. The geometric accuracy calculation process is carried out for all five LiDAR datasets, where each LiDAR dataset has 16 checkpoints scattered in the corresponding LiDAR dataset. The location of the checkpoints is determined on a horizontal area located on the ground and not obstructed by vegetation or man-made objects. Table 6 shows the RMSE results of geometric accuracy in the LiDAR data filtering results for the three methods.

DOI: https://doi.org/10.17509/gea.v25i1.71587
p-ISSN 1412-0313 e- ISSN 2549-7529

**Table 6.** RMSE of Geometric Accuracy From Each Filtering Method

| Dataset | ATIN | | CSF | | PMF | |
|---|---|---|---|---|---|---|
| | Min | Max | Min | Max | Min | Max |
| 1 | 0.09 | 0.436 | 0.318 | 0.59 | 0.011 | 0.431 |
| 2 | 0.0098 | 0.331 | 0.0021 | 0.738 | 0.013 | 0.382 |
| 3 | 0.005 | 0.219 | 0.042 | 0.347 | 0.011 | 0.323 |
| 4 | 0.0007 | 0.034 | 0.0035 | 0.297 | 0.0009 | 0.055 |
| 5 | 0.033 | 0.429 | 0.016 | 0.689 | 0.03 | 0.504 |

Through the data presented in Table 6, it can be seen that the ATIN method as a whole has the smallest RMSE, followed by the PMF method and the CSF method. The smallest average RMSE is obtained in Dataset 4 which has characteristics of hill areas and rice fields, while the largest average RMSE is obtained in Dataset 1 with characteristics of hill areas and factories. Furthermore, the calculation of the standard deviation value of geometric accuracy results can be seen in Table 7.

**Table 7.** Standard Deviation of Geometric Accuracy Results

| Dataset | Standard Deviation of Geometric Accuracy | | |
|---|---|---|---|
| | ATIN | CSF | PMF |
| 1 | 0.1017 | 0.0874 | 0.1142 |
| 2 | 0.0965 | 0.1691 | 0.1137 |
| 3 | 0.0723 | 0.0863 | 0.0838 |
| 4 | 0.0104 | 0.0741 | 0.0162 |
| 5 | 0.1048 | 0.1596 | 0.1197 |

The filtering process is not free from point classification errors, so it is not uncommon to find errors in point classification, where points that should be classified into non-soil objects are detected as land objects. The point classification error may be caused by an inaccuracy in the selection of parameter composition, where the parameters used in the LiDAR data filtering process are still not in accordance with the characteristics of LiDAR data. The fewer point classification errors that occur in the filtering process, the better the quality and accuracy of the parameter composition used and the filtering algorithm used in LiDAR point cloud data. The combination of parameter values in Table 1 was selected based on the results of trial and error and refers to the parameter values of previous research (Cai et al., 2023; Chen et al., 2021).

DOI: https://doi.org/10.17509/gea.v25i1.71587
p-ISSN 1412-0313 e- ISSN 2549-7529

Through the visualization in Table 2, it can be seen that the filtering results using the ATIN method are relatively good, marked by vegetation objects and man-made objects such as buildings not appearing in the filtering results. This indicates that vegetation objects and man-made objects can be well described as non-soil objects, successfully filtered and not included in the soil object class. The topographical details of the land surface are well preserved and minimized from misclassification.

The filtering results using the CSF method have a dense density of points in flat areas. However, if the dataset conditions have special characteristics, namely the presence of appearances with significant elevation changes such as hills, then the density of points in the relief area will decrease significantly. Even in some datasets that have been tested, such as in a fairly large hilly relief area, there are no ground points that represent the topographic conditions of the area because it is located in a sloping or steep area. This is one of the limitations of the CSF method, which is not able to perform the filtering process well in areas with relief or steep topographic conditions.

In Table 2, it also can be seen that overall, the PMF method can remove non-soil objects such as vegetation objects and man-made objects such as buildings successfully. However, when compared to the filtered data using the ATIN and CSF methods, it is quite visible that the PMF method filtered data has a larger distance between points than the filtering results using the other two methods. This is because the number of remaining points in the filtered data is significantly reduced, so the distance between points in the filtered data looks more tenuous.

After calculating the filtering results, the ATIN method has a fairly high percentage of filtered points, which is in the range of 70% to 84.5%. Based on the visualization of the filtering results and also the percentage of filtered points, it can be seen that the ATIN method has succeeded in filtering LiDAR data well because it is able to correctly classify land and non-soil objects and has a good and evenly distributed point density. The CSF method has a fairly low percentage of filtered points, which is in the range of 44% to 66%. This causes many points to be detected as soil objects when compared to the other two filtering methods. However, the points classified as land objects still cannot represent the topographic conditions of each dataset as a whole due to the shortcomings of the CSF method to perform the object classification and filtering process in areas with non-flat topographic conditions. Meanwhile, the PMF method has the highest percentage of filtered points, which is in the range of 94% to 95%. The high percentage of filtered points causes the density of points in the dataset to decrease significantly. As a result, the filtering results of the PMF method are not able to capture the details in the data as in the other two filtering methods, even though the distribution of land object points is good and evenly distributed.

The DTM extraction results have a fairly high resolution of 2 meters. This shows that LiDAR point cloud data can produce DTM surfaces with high resolution. DTM with a resolution of 2 meters can be used to create maps with a scale of up to 1: 4000. It can be seen that in some DTM extraction results, there are some empty parts that are white in color. This can be caused by a lack of point density at certain locations in the dataset. Point density is one of the important things to maintain in the DTM extraction process because if a dataset has a tight and even point density, the interpolation process carried out to form a DTM will produce a continuous surface and can avoid interpolation failure. Interpolation failure causes the DTM surface to have missing or empty areas and is not continuous. One of the main factors that cause interpolation failure is the lack or absence of points that represent an area at a certain distance.

The DTM extraction results of the ATIN method have good quality. This can be seen from the level of detail of the DTM extraction results, where the ATIN method DTM extraction results have a fairly high level of detail. However, the DTM extraction results of the ATIN method have some small missing or empty parts, especially in areas that have many buildings such as those in the DTM representation of dataset 1. This is supported by the results of research conducted by (Raj et al., 2024) which found that the ATIN algorithm tends to be difficult to filter discontinuous surfaces such

DOI: https://doi.org/10.17509/gea.v25i1.71587
p-ISSN 1412-0313 e- ISSN 2549-7529

as urban areas or areas with many buildings. This is because the ATIN algorithm tends to eliminate the base of the building because the threshold value is passed. So, in this study it is again proven that the ATIN algorithm is less able to perform the filtering process optimally in areas that have many buildings, although overall almost all DTM surfaces can be interpolated properly.

DTM extraction results from LiDAR point cloud data filtering results using the CSF method show a good level of detail. This can be seen from the texture contained in the DTM extraction results which are quite detailed. However, in the DTM extraction results of LiDAR data filtering using the CSF method, there are also weaknesses, namely the number of empty or missing areas from the DTM surface, especially in areas with high topographic variations. This is caused by the less than optimal CSF filtering algorithm on LiDAR point cloud data when used in areas with high topographic variations. This is discussed in research conducted by Chen et al. (2021), where the CSF algorithm is less suitable for areas with complex topographic features, such as relief and steep areas. This issue is evident in the DTM extraction results from the CSF method in this study, particularly in hilly areas with steep slopes, such as in datasets 1 and 4, the Binning method used for DTM generation in this study was unable to interpolate some parts of the area contained in the hilly area. The failure of the interpolation process causes some parts contained in the DTM representation of the CSF method to be empty or missing. In research conducted by (Chen et al., 2021) it is also mentioned that the CSF algorithm is suitable for use in flat areas. This has also been proven true in this study, where from the resulting DTM representation, flat areas such as rice fields can almost entirely be well interpolated into DTM surfaces using the Binning algorithm. This indicates that the density of points in the rice field area has been spread evenly so that the interpolation process can be done well.

In the DTM extraction results from LiDAR point cloud data filtering results using the PMF method, the resulting DTM surface as a whole can be interpolated properly. This is indicated by the absence of missing or empty parts in the DTM extraction results. The PMF method has successfully performed the filtering process well, where all points included in the ground points can be spread evenly so that the interpolation process can be done thoroughly. However, when referring back to Table 3, the percentage of filtered points is very high, reaching 95%. The high percentage of filtered points also causes weaknesses and shortcomings in the DTM extraction results of the PMF method, namely the lack of detail in the resulting DTM representation. The poor level of detail in the DTM extraction results of the PMF method is due to the lack of point density in the entire area, so there are not enough points to represent the existing topographic details, even though the ground points are evenly distributed. In addition, the DTM extraction results from the filtered dataset using the PMF method have not been able to remove non-soil objects as well as the other two methods. This is evident in the DTM representation of the PMF method where it can be seen that there are still some non-soil objects such as trees included in the DTM surface.

The geometric accuracy value that can be seen in Table 6 shows that the ATIN method has the best geometric accuracy value in dataset 4 which has the characteristics of rice fields and hills, with a height difference between the check point and LiDAR data of 0.0007 meters. The worst geometric accuracy of the ATIN method, which is 0.436 meters, is found in dataset 1 with the characteristics of industrial and hilly area datasets.

Then in the CSF method, the best geometric accuracy value is obtained in a flat area in dataset 2 which is 0.0021 meters. While the worst geometric accuracy of 0.738 meters is also found in dataset 2 but in areas that have relief variations. This can occur due to less ideal selection of checkpoint locations or the absence of points in the filtered data that represent the height in the check point area. The results of this geometric accuracy prove that the CSF algorithm has a weakness when faced with datasets that have topographic relief characteristics or steep slopes because it is likely to have low geometric accuracy. This is because the fabric simulation is prone to errors in sloping or steep

DOI: https://doi.org/10.17509/gea.v25i1.71587
p-ISSN 1412-0313 e- ISSN 2549-7529

areas. Due to this limitation, the CSF algorithm becomes less flexible when filtering LiDAR data, especially in areas that are not flat.

The geometric accuracy value produced by LiDAR point cloud data filtering results using the PMF method has quite good results and is almost close to the geometric accuracy produced by the ATIN method. The best accuracy obtained by the PMF method was obtained in dataset 4 with an accuracy of 0.0009 meters. The accuracy was obtained in a flat area, namely rice fields. Meanwhile, the worst accuracy obtained by the PMF method is in dataset 5 with an accuracy of 0.504 meters. This can happen because there is no point in the filtered data that represents the height in the checkpoint area.

Through the calculation of the standard deviation of geometric accuracy results contained in Table 7, it can be seen that the overall dataset that has gone through the filtering process using the ATIN method produces the smallest standard deviation value when compared to the other two filtering methods. The PMF method has a slightly larger standard deviation value than the ATIN method, while the CSF method has the largest standard deviation value. This indicates that the ATIN method can perform the filtering process with even quality for various conditions.

## 4. CONCLUSIONS

From the findings of the research, overall the ATIN method produces better results when compared to the CSF method and the PMF method. This is determined based on several factors, where the ATIN method has the fastest processing time with the best accuracy rate. The CSF method has data with the highest point density, but the lowest accuracy rate. Meanwhile, the PMF method has data with the lowest point density, the longest processing time, but has a fairly good accuracy rate. The filtering process using the three methods has its own advantages and disadvantages. The ATIN filtering method works well in study areas that have topographic variations and flat areas such as hills and rice fields, but not well for urban areas or areas with many buildings. The CSF filtering method works well on study areas that are in flat areas such as urban areas and rice fields, but less well for complex areas and have topographic variations. The PMF filtering method works well on areas with topographical variations as well as flat areas, but its tendency to remove many points during the filtering process causes the DTM extraction results to be less detailed than the ATIN method and the CSF method.

## 5. RECOMMENDATIONS

Future research should focus on refining the parameter settings for each filtering algorithm to enhance their adaptability to diverse terrain characteristics. Specifically, optimizing the CSF method for areas with significant elevation changes could improve its applicability. Additionally, combining the strengths of different methods might yield more robust filtering algorithms capable of maintaining high point density and geometric accuracy across various landscapes. Implementing machine learning techniques to dynamically adjust parameters based on terrain features could also be a promising direction to enhance LiDAR data processing and DTM accuracy.

## 6. REFERENCES

Anand, B., Senapati, M., Barsaiyan, V., and Rajalakshmi, P. (2021). LiDAR-INS/GNSS-based real-time ground removal, segmentation, and georeferencing framework for smart transportation. *IEEE Transactions on Instrumentation and Measurement*, 70, 1-11.

Asy'ari, M., Syam'ani, S. A., dan Satriadi, T. (2022). Estimasi biomassa tegakan hutan hujan tropis di bukit mandiangin menggunakan metode interpolasi spasial. *Jurnal Hutan Tropis*, *10*(3), 315-328.

DOI: https://doi.org/10.17509/gea.v25i1.71587
p-ISSN 1412-0313 e- ISSN 2549-7529

Bailey, G., Li, Y., McKinney, N., Yoder, D., Wright, W., and Herrero, H. (2022). Comparison of ground point filtering algorithms for high-density point clouds collected by terrestrial LiDAR. *Remote Sensing*, *14*(19), 4776.

Cai, S., Yu, S., Hui, Z., and Tang, Z. (2023). ICSF: An improved cloth simulation filtering algorithm for airborne LiDAR data based on morphological operations. *Forests*, *14*(8), 1520.

Chen, C., Guo, J., Wu, H., Li, Y., and Shi, B. (2021). Performance comparison of filtering algorithms for high-density airborne LiDAR point clouds over complex landscapes. *Remote Sensing*, *13*(14), 2663.

Fareed, N., Flores, J. P., and Das, A. K. (2023). Analysis of UAS-LiDAR ground points classification in agricultural fields using traditional algorithms and point CNN. *Remote Sensing*, *15*(2), 483.

Hidayat, H., dan Sudarsono, P. A. K. (2024). Analisis pembuatan kontur peta rupa bumi indonesia dengan wahana LiDAR (light detection and ranging) (studi kasus: penajam, kalimantan timur). *GEOID*, *19*(2), 274-282.

Khan, N. R., and Kumar, S. V. (2024). Terrestrial LiDAR derived 3D point cloud model, digital elevation model (DEM) and hillshade map for identification and evaluation of pavement distresses. *Results in Engineering*, 23, 102680.

Kim, H., Lee, J., and Kim, Y. (2021). Tidal creek mapping from airborne LiDAR data using multi-resolution cloth simulation filtering. *Journal of Coastal Research*, 114(SI), 86-90.

Kim, I., Martins, R. J., Jang, J., Badloe, T., Khadir, S., Jung, H. Y., ... and Rho, J. (2021). Nanophotonics for light detection and ranging technology. Nature nanotechnology, 16(5), 508-524.

Kuçak, R. A., and Büyüksalih, İ. (2023). Comparison of CSF ground filtering method by using airborne LiDAR data. *Advanced LiDAR*, *3*(2), 47-52.

Li, H., Ye, C., Guo, Z., Wei, R., Wang, L., and Li, J. (2021). A fast progressive TIN densification filtering algorithm for airborne LiDAR data using adjacent surface information. *IEEE Journal of Selected Topics in Applied Earth Observations and Remote Sensing*, 14, 12492-12503.

Lin, Y. C., Manish, R., Bullock, D., and Habib, A. (2021). Comparative analysis of different mobile LiDAR mapping systems for ditch line characterization. *Remote Sensing*, *13*(13), 2485.

Lopac, N., Jurdana, I., Brnelić, A., and Krljan, T. (2022). Application of laser systems for detection and ranging in the modern road transportation and maritime sector. *Sensors*, *22*(16), 5946.

Oniga, V. E., Loghin, A. M., Macovei, M., Lazar, A. A., Boroianu, B., and Sestras, P. (2023). Enhancing LiDAR-UAS derived digital terrain models with hierarchic robust and volume-based filtering approaches for precision topographic mapping. *Remote Sensing*, *16*(1), 78.

Raj, P. P. C., Rahman, M. Z. A., Ariffin, A., Kadir, W. H. W., and Suhaili, H. (2024). Integration of different density UAV lidar and single beam echo sounder (SBES) for river and riparian area digital derrain model (DTM) construction. *Journal of Advanced Geospatial Science and Technology*, *4*(1), 106-129.

Ramadhan, A. S., Cahyono, A. B., dan Hariyanto, T. (2024). Analisis pemodelan tiga dimensi candi gunung gangsir menggunakan low-cost LiDAR dan terrestrial laser scanner. *GEOID*, 19(3), 519-528.

Samodra, G. (2022). Simulasi morfodinamika longsor kalisari, kabupaten magelang berdasarkan data lidar dan model numerik. *Jurnal Lingkungan dan Bencana Geologi*, *13*(2).

Štroner, M., Urban, R., Lidmila, M., Kolář, V., and Křemen, T. (2021). Vegetation filtering of a steep rugged terrain: the performance of standard algorithms and a newly proposed workflow on an example of a railway ledge. *Remote Sensing*, *13*(15), 3050.

Wang, T., Deng, L., Li, Y., and Peng, H. (2021). Progressive TIN densification with connection analysis for urban LiDAR data. *Photogrammetric Engineering & Remote Sensing*, *87*(3), 205-213.

DOI: https://doi.org/10.17509/gea.v25i1.71587
p-ISSN 1412-0313 e- ISSN 2549-7529

Yu, D., He, L., Ye, F., Jiang, L., Zhang, C., Fang, Z., dan Liang, Z. (2022). Unsupervised ground filtering of airborne-based 3D meshes using a robust cloth simulation. *International Journal of Applied Earth Observation and Geoinformation*, 111, 102830.

Zheng, J., Xiang, M., Zhang, T., and Zhou, J. (2024). An improved adaptive grid-based progressive triangulated irregular network densification algorithm for filtering airborne LiDAR data. *Remote Sensing*, *16*(20), 3846.

DOI: https://doi.org/10.17509/gea.v25i1.71587
p-ISSN 1412-0313 e- ISSN 2549-7529